shaped curve initiates transition to the alternative branch. The system returns to the stationary state only after a very long excursion, following a circumferential route along both branches, as seen in the figure. In the case shown in Fig. 1.5c, both stationary states are excitable, and the system switches between them following a weak perturbation. A much stronger perturbation is needed to initiate a switch when the null-isoclines are arranged as in Fig. 1.5d.

1.4.3 Almost Hamiltonian Dynamics

Global bifurcations can be studied analytically with the help of the amplitude equations (normal forms) obtained as an unfolding of the TB bifurcation (Sect. 1.3.5). We have seen that these equations can take the form of perturbed Hamiltonian systems with weakly dissipative corrections. We shall rewrite (1.85) as

$$\dot{x} = y, \qquad \dot{y} = f(x) + \delta\, y\, g(x), \tag{1.89}$$

where $f(y)$, $g(y)$ are, respectively, nth and mth order polynomials and δ is a small parameter.

At $\delta = 0$, the system is conservative. The conserved quantity is "energy"

$$E = \tfrac{1}{2}y^2 + V(x), \qquad V(y) = -\int f(x)\,\mathrm{d}x. \tag{1.90}$$

The minima of the potential $V(x)$ correspond to stable stationary states and the maxima to saddle points. The equation of motion can be obtained by varying the action integral

$$S = \int \left[\tfrac{1}{2}y^2 - V(x)\right]\,\mathrm{d}t. \tag{1.91}$$

Equation (1.89) at $\delta = 0$ can be easily resolved by eliminating time to obtain trajectories in the phase plane spanned by x and its time derivative (or "momentum" y):

$$y^2 = 2[E - V(x)]. \tag{1.92}$$

Trajectories at different levels of E may be qualitatively different (see Fig. 1.7). At low energies, each trajectory surrounds one of stable stationary states only; at energies exceeding those of both stationary states, the level $E = \mathrm{const}$ would consist of two disconnected parts. At high energies, each trajectory surrounds both stable stationary states. The boundary between the two types corresponds to the energy of the intermediate unstable state. This is a homoclinic trajectory passing through the unstable state.

At $\delta \neq 0$, the energy changes with time:

$$\dot{E} = \frac{\partial E}{\partial x}\,\dot{x} + \frac{\partial E}{\partial y}\,\dot{y} = \delta\, y^2 g(x). \tag{1.93}$$

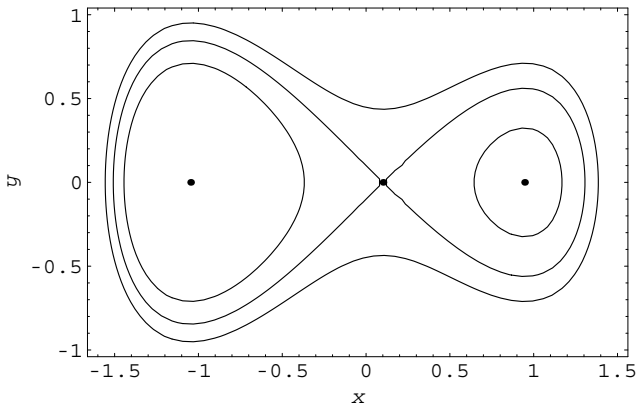

Fig. 1.7. Trajectories of a Hamiltonian system with two stable fixed points

When δ is small, the energy changes slowly, so that it remains nearly constant during an oscillation period T along a particular trajectory. We can then compute the rate of change of energy by averaging over the period T:

$$\langle \dot{E} \rangle \equiv \frac{\Delta E}{T} = \frac{\delta}{T} \int_t^{t+T} y^2 g(x)\,\mathrm{d}t = \delta \int_{x_{\min}}^{x_{\max}} y(x) g(x)\,\mathrm{d}x \Big/ \int_{x_{\min}}^{x_{\max}} \frac{\mathrm{d}x}{y(x)} \tag{1.94}$$

The integration limits in the last integrals are values of x at turning points where y vanishes, i.e., the suitable roots of $E = V(x)$.

For a specific system, the computed "dissipation rate" $\Delta E/T$ can be expressed as a function of energy[7], and may vanish on a certain trajectory. We can observe that even arbitrarily weak dissipation brings about a qualitative change of dynamic behavior. A conservative system can move along any available trajectory, depending on its energy. On the contrary, a weakly dissipative system evolves to a certain energy level where the average change of energy vanishes. A trajectory becomes stationary when the dissipation integral vanishes:

$$\int_{x_{\min}}^{x_{\max}} y(x) g(x)\,\mathrm{d}x = \sqrt{2} \int_{x_{\min}}^{x_{\max}} g(x) \sqrt{E - V(x)}\,\mathrm{d}x = 0. \tag{1.95}$$

1.4.4 Bifurcation Diagrams

In order to construct a global bifurcation diagram, we have to focus attention on the values of parameters when special (nongeneric) trajectories, such

[7] Dissipation, of course, can be negative only in a system sustained far from equilibrium. Then it is sometimes called "antidissipation".

as homoclinics, become stationary. Strictly speaking, the above derivation, assuming that the energy change during a single oscillation period is small, fails for an infinite-period homoclinic trajectory. Nevertheless, the stationarity condition for a homoclinic trajectory correctly indicates the location of the saddle-loop bifurcation in a weakly dissipative system of the type (1.89).

As an example, consider (1.89) with a cubic $f(x)$ and quadratic $g(x)$:

$$f(x) = \mu_0 + x - x^3, \qquad g(x) = \mu_1 + \mu_2 x - x^2. \tag{1.96}$$

The roots of $f(x) = 0$ are two stable fixed points $x_s^{\pm}$ and the unstable one x_s^0; they can be found explicitly using a convenient trigonometric expression for the roots of a cubic polynomial:

$$\begin{aligned} x_s^{\pm} &= -(2/\sqrt{3})\sin(\psi \mp \pi/3), \qquad x_s^0 = (2/\sqrt{3})\sin\psi, \\ \psi &= \tfrac{1}{3}\arcsin(\tfrac{3}{2}\sqrt{3}\mu_0). \end{aligned} \tag{1.97}$$

Local analysis gives immediately the location of a saddle-node bifurcation $\mu_0 = 2/3^{3/2}$. The condition for Hopf bifurcation on the branches of fixed points $y = 0,\ x = x_s^{\pm}(\mu_0)$ is $g(x_s^{\pm}) = 0$. In order to determine whether this bifurcation is supercritical or subcritical, one can obtain an analytic approximation of the dissipation integral for small-amplitude orbits with E slightly above $V(x_s^{\pm})$ taking into account that these orbits are almost harmonic.

The homoclinic orbit corresponds to the energy level $E = V(x_s^0)$. It is shaped as the figure eight, with its two loops surrounding each of stable fixed points. The stationarity condition (1.95) evaluated separately for each loop defines $\mathrm{sl}^{\pm}$ bifurcation on the branch of periodic orbits surrounding the respective point, while the condition evaluated for the entire figure-eight defines sl^0 bifurcation on the branch of "large" orbits surrounding all three fixed points.

Figure 1.8a shows a 2D section of the bifurcation diagram in the 3D parametric space for a typical value $\mu_0 = 0.1$ in the domain where three fixed points exist. The loci of Hopf and saddle-loop bifurcations in the parametric plane μ_1, μ_2 are straight lines, and each fixed point is stable to the left of the respective Hopf locus. The snp loci are not shown in this figure, but one involving "large" orbits is seen in Fig. 1.8b, which presents a blow-up near the intersection of the three sl lines.

One can observe that the loci of Hopf and $\mathrm{sl}^{\pm}$ bifurcations intersect (as they also do in Fig. 1.4), so that at positive and weakly negative values of μ_1 the saddle-loop bifurcation occurs while the fixed point is still stable. This suggests that the Hopf bifurcation might be subcritical at these values of the parameters and the sl bifurcation takes place on the branch of unstable periodic orbits. This is not precisely so, since the intersection of these loci has no particular significance, while the dynamically important codimension two points in the parametric space are those where the third-order coefficient in the expansion at Hopf bifurcation vanishes (DH) and where the homoclinic orbit is neutrally stable (NSL). These points do not generically coincide and should be connected by an snp branch. The snp loci (not discernable on the